

Transient dynamics in altered disturbance regimes: recovery may start quickly, then slow

Robin E. Snyder

Received: 28 July 2008 / Accepted: 21 October 2008 / Published online: 15 November 2008
© Springer Science + Business Media B.V. 2008

Abstract When a pattern of spatial or temporal environmental variation changes, it takes time for populations to reach their new stationary distributions, and during this time, the competitive landscape is also in flux. As a first step toward understanding community responses to altered variational regimes, I investigate the convergence of an annual–perennial plant system to its stationary spatiotemporal distribution following a change in environmental variation. I find that, to good approximation, convergence is the sum of two separate processes: global convergence, which governs changes in the total population, and local convergence, which governs population redistribution. While the slower process (global or local) eventually governs convergence, the faster process may initially dominate if it starts further from its stationary distribution, so that the populations converge quickly at first, then slow down. That is, when disturbances are spatially heterogeneous, a system may be initially more resilient under some initial conditions than others.

Keywords Transient dynamics · Resilience · Spatiotemporal · Altered disturbance regime · Annual · Perennial

Introduction

Many communities are believed to be maintained by disturbance (e.g., Abrams 1982; Litvaitis 2001; Dettmers 2003) or other forms of environmental variation (e.g., Chesson et al. 2004; Adler et al. 2006), but disturbance regimes are increasingly being altered as the result of global climate change (USGCRP 2000), invasive species that act as “ecosystem engineers” (Mack and D’Antonio 1998), or policy changes (e.g., in fire suppression practices). Theoretical work on coexistence in variable environments (Chesson 1994, 2000; Snyder and Chesson 2004; Snyder 2008) can help predict whether species will continue to coexist in the new disturbance regime and how they will be distributed, but this work has focused on long-term dynamics. When a disturbance regime or any other pattern of environmental variation changes, it takes time for populations to reach their new stationary distributions, and during this time, the competitive landscape is also in flux.

This transition period between one stationary distribution and another can be especially important for plants, whose population dynamics are especially sensitive to spatial structure (Silvertown et al. 1992; Rees et al. 1996; Law and Dieckmann 2000; Stoll and Prati 2001; Turnbull et al. 2007). Furthermore, changes in vegetative distribution can change the structure of associated animal communities (Weller and Spratcher 1965), and because of the effects on both plant and animal communities, it has been argued that the spatial distribution of plant communities should be considered when evaluating restoration success (Seabloom and van der Valk 2003).

This article is intended as a Letter.

R. E. Snyder (✉)
Department of Biology, Case Western Reserve University,
10900 Euclid Ave., 44106-7080 Cleveland, OH, USA
e-mail: res29@case.edu

How long do these transient dynamics last? How quickly can a community adjust to a change in environmental variation? On a more applied note, how soon should we expect to see the long-term results of reinstating a historical disturbance regime? How long should we monitor environmental impacts after changing a disturbance regime?

As a first step toward understanding community responses to altered variational regimes, this paper investigates the convergence of an annual–perennial plant system to its stationary spatiotemporal distribution following a change in the pattern of environmental variation. I find that, to good approximation, convergence is the sum of two separate processes: global convergence and local convergence. Global convergence is the convergence of the total population (alternatively, the spatially averaged population) to its eventual level. Local convergence is the redistribution of the population to its eventual pattern of high- and low-density areas, relative to the current spatial average. The full convergence rate is eventually determined by whichever process is slower, yet, depending on initial conditions, the faster process may initially dominate. In such a case, convergence is relatively rapid at first, then slows. I present calculations for the global and local convergence rates and discuss the conditions under which the faster process may initially dominate. These calculations are also appropriate for analyzing a system's recovery rate after a single disturbance, a quantity often called resilience (*sensu* Webster et al. 1975; Beddington et al. 1976; Harrison 1979). Considered from this perspective, this paper finds that, when disturbances are spatially heterogeneous, resilience depends on initial conditions.

Model

The number of annual *seeds* at location x in year t is $n_a(x, t)$, while the number of perennial *adults* is $n_p(x, t)$. Seeds germinate with probability g_j ($j = a, p$) and, upon establishing themselves as adult plants, produce at most $E_j(x, t)$ seeds (“fecundity”), which varies spatially and temporally as a result of fluctuating environmental conditions. I represent fecundity by E_j as a reminder that fecundity is determined by environmental conditions and will refer to fecundity as the “environment,” even though, technically, it is a response to the environment. Actual seed production is reduced by competition, C_j . The seeds then disperse, traveling a distance z from their parent with probability $k_j(z)$. Annual seeds that fail to germinate survive with probability s_a until the following year, when they again have a chance to

germinate. Perennial adults survive until the following year with probability s_p . Thus,

$$n_a(x, t+1) = \int_{-\infty}^{\infty} k_a(x-y) \left(\frac{E_a g_a n_a}{C_a} \right) (y, t) dy + s_a(1 - g_a)n_a(x, t) \quad (1)$$

$$n_p(x, t+1) = g_p \int_{-\infty}^{\infty} k_p(x-y) \left(\frac{E_p n_p}{C_p} \right) (y, t) dy + s_p n_p(x, t), \quad (2)$$

Competition depends on a weighted average of the local populations, with weight function U_{jk} (“competition kernel”) defined so that more distant neighbors have less of a competitive effect:

$$C_a(x, t) = \int_{-\infty}^{\infty} \gamma_{ap} U_{ap}(x-y) n_p(y, t) dy + \int_{-\infty}^{\infty} \gamma_{aa} U_{aa}(x-y) g_a n_a(y, t) dy$$

$$C_p(x, t) = \int_{-\infty}^{\infty} \gamma_{pp} U_{pp}(x-y) n_p(y, t) dy + \int_{-\infty}^{\infty} \gamma_{pa} U_{pa}(x-y) g_a n_a(y, t) dy. \quad (3)$$

The γ coefficients account for the different competitive effects that annuals and perennials have on each other. Adult perennials are generally immune to competition from annuals; however, perennial seedlings still experience competition from annual seedlings. This extra source of competition is represented by letting γ_{pa} be small but nonzero.

I used Laplacian dispersal and competition kernels to generate the figures: $k_j(z) = \exp(-|z|/a_j)/(2a_j)$ and $U_{jk} = \exp(-|z|/b_{jk})/(2b_{jk})$. Thus, the mean dispersal distance for species j is a_j , and competition between species j and k is significant over a distance b_{jk} .

Loosely inspired by California grasslands, I let the mean annual fecundity ($\langle E_a \rangle_{x,t}$) be 200, mean perennial fecundity ($\langle E_p \rangle_{x,t}$) be 45, and perennial survival (s_p) be 0.5 (for a mean lifetime of 3 years) (Seabloom et al. 2003; Borer et al. 2007). Germination rates and the competition coefficients were then set so as to ensure coexistence, with annual germination (g_a) equal to 0.5, perennial germination (g_p) equal to 0.9, $\gamma_{pp} = \gamma_{ap} = 1$, $\gamma_{aa} = 0.6$, and $\gamma_{pa} = 0.2$. This choice for the competition coefficients is consistent with the finding that competition imposed on annuals by other annuals is less than competition imposed on annuals by adult perennials (Borer et al. 2007).

In the figures, theoretical predictions are compared against convergence rates obtained by numerically integrating the full model equations. When numerically

integrating, the spatial domain is 1,024 units long, which is always an integral multiple of the spatial period of the environmental variation. Circular boundary conditions were used (i.e., the two ends of the domain were treated as adjacent).

A word on units: the unit of time is 1 year (hence, there is no survival term for adult annuals). I take the unit of space to be the radius of an average plant, so that, with a leptokurtic dispersal kernel such as the one used here, a mean dispersal distance of 2 represents short-range dispersal: 46% of the seeds fall within two “plant radii” from the center of their parent. A mean dispersal distance of 10 represents long-distance dispersal: only 1.5% fall within the two plant radii of their parent’s center.

Analysis

The key to analyzing the transient dynamics is to assume small fluctuations, linearize the model, and take the spatial Fourier transform. This causes what would otherwise be an intractable spatiotemporal process to decompose into independent matrix models for each spatial frequency—i.e., for each spatial scale at which variation is present.

Let us write the local population of species j , $n_j(x, t)$, and the spatially averaged population, $\langle n_j \rangle_x(t)$, in terms of $O(\sigma)^1$ perturbations $u'_j(x, t)$ and $\eta'_j(t)$:

$$\begin{aligned} \langle n_j \rangle_x(t) &= \langle n_j \rangle_{x,t}(1 + \eta'_j(t)) \\ n_j(x, t) &= \langle n_j \rangle_x(t)(1 + u'_j(x, t)) \\ &= \langle n_j \rangle_{x,t}(1 + u'_j(x, t) + \eta'_j(t)) + O(\sigma^2). \end{aligned} \tag{4}$$

In theory, spatial and temporal averages are taken across all space and all time, though in practice, they would be taken across one period in a periodic system or across distances and times much larger than the spatial and temporal correlation lengths in a stochastic system. The perturbation $\eta'_j(t)$ represents the deviation of the spatially averaged population, $\langle n_j \rangle_x(t)$, from the spatially and temporally averaged population, $\langle n_j \rangle_{x,t}$, and η'_j ’s convergence to a stationary distribution represents the global convergence of the spatially averaged or total population to its new spatiotemporal mean. The perturbation $u'_j(x, t)$ represents the deviation of

the local population from the spatial average, and u'_j ’s convergence to a stationary distribution represents the local redistribution of the population in accordance with the new pattern of variation. Similarly, the environmental response $E_j(x, t)$ (representing fecundity, survival—whatever is varying in response to fluctuating environmental conditions) can be written in terms of $O(\sigma)$ fluctuations ϵ_j and Ω_j :

$$\begin{aligned} \langle E_j \rangle_x(t) &= \langle E_j \rangle_{x,t}(1 + \Omega_j(t)) \\ E_j(x, t) &= \langle E_j \rangle_x(t)(1 + \epsilon_j(x, t)) \\ &= \langle E_j \rangle_{x,t}(1 + \epsilon_j(x, t) + \Omega_j(t)) + O(\sigma^2). \end{aligned} \tag{5}$$

Next, we linearize the model equations about $\langle n_j \rangle_{x,t}$ and $\langle E_j \rangle_{x,t}$ and take the spatial Fourier transform, so that the dynamics of n_j are reexpressed as the dynamics of $\eta'_j(t)$ and $\tilde{u}'_j(q, t)$, where $\tilde{u}'_j(q, t)$ is the spatial Fourier transform of $u'_j(x, t)$. By taking the Fourier transform of $u'_j(x, t)$, we are reexpressing $u'_j(x, t)$ as a sum of sine waves, where $\tilde{u}'_j(q, t)$ is the coefficient of the sine wave at spatial frequency q (period $2\pi/q$). The quantity $\tilde{u}'_j(q, t)$ thus represents the amount of variation present in $u'_j(x, t)$ at frequency q . Making u'_a and u'_p the components of a vector, $\tilde{\mathbf{u}}'$, and likewise with η'_a and η'_p , the linearized dynamics become

$$\begin{aligned} \tilde{\mathbf{u}}'(q, t + 1) &= \mathbf{B}_u(q)\tilde{\mathbf{u}}'(q, t) + \mathbf{B}_\epsilon(q)\tilde{\boldsymbol{\epsilon}}(q, t) \\ \boldsymbol{\eta}'(t + 1) &= \mathbf{B}_\eta\boldsymbol{\eta}'(t) + \mathbf{B}_\Omega\boldsymbol{\Omega}(t), \end{aligned} \tag{6}$$

where the components of $\mathbf{B}_u(q)$, \mathbf{B}_η , $\mathbf{B}_\epsilon(q)$, and \mathbf{B}_Ω come from the linearized model equations (see the [Appendix](#)).

In the absence of environmental variation, the populations would come to an equilibrium, constant in space and time, but external forcing causes the population to vary in a characteristic pattern. This eventual pattern, determined by the form of the environmental variation, is the stationary distribution. A more traditional way to analyze this system would be to linearize about the stationary distribution. However, this leaves us with coefficients that still vary in time and space, which renders the Fourier transform useless and leaves the dynamics at different spatial scales coupled. Numerical evidence shows that linearizing about the spatiotemporal averages of n_j and E_j allows for good predictions of the stationary distribution under most circumstances (see, for example, Snyder 2007), and the convergence properties are well predicted, as is shown by the figures in this paper. That is, the stationary distribution for the linearized system is close to that for the nonlinear system, and the convergence properties of the two are similar. This form of linearization yields less accurate results when the population varies strongly in response

¹By “ $g(x)$ is $O(\sigma)$,” I mean that $g(x)$ decreases rapidly enough with σ that $\left| \frac{g(x)}{\sigma} \right|$ can be made less than or equal to some positive constant K for σ small enough. Here, σ is not a model parameter but rather a bookkeeping device used to ensure a consistent order of approximation.

to environmental variation because these conditions violate the assumption of small fluctuations. Even then, however, we can still achieve good convergence predictions by adjusting $\langle n_j \rangle_{x,t}$, as is discussed at the end of this section.

Let us write $\tilde{\mathbf{u}}(q, t)$ as the (linearized) stationary distribution, $\tilde{\mathbf{u}}_s(q, t)$, plus a transient portion, $\tilde{\mathbf{u}}(q, t)$, and similarly, $\boldsymbol{\eta}'(t) = \boldsymbol{\eta}_s(t) + \boldsymbol{\eta}(t)$. By definition, $\tilde{\mathbf{u}}_s(q, t+1) = \mathbf{B}_u(q)\tilde{\mathbf{u}}_s(q, t) + \mathbf{B}_\epsilon(q)\tilde{\boldsymbol{\epsilon}}(q, t)$ and $\boldsymbol{\eta}_s(t+1) = \mathbf{B}_\eta\boldsymbol{\eta}_s(t) + \mathbf{B}_\Omega\boldsymbol{\Omega}(t)$. Thus,

$$\begin{aligned}\tilde{\mathbf{u}}(q, t+1) &= \mathbf{B}_u(q)\tilde{\mathbf{u}}(q, t) \\ \boldsymbol{\eta}(t+1) &= \mathbf{B}_\eta\boldsymbol{\eta}(t),\end{aligned}\quad (7)$$

where the elements of $\mathbf{B}_u(q)$ and \mathbf{B}_η are given in the [Appendix](#).

For now, let us consider sinusoidal variation at a single spatial scale (i.e., $E_j(x, t) - \langle E_j \rangle_{x,t} \propto \sin(qx)f(t) + g(t)$, where $\langle f(t) \rangle_t = \langle g(t) \rangle_t = 0$), so that $\mathbf{n}(x, t)$ can be represented by a single Fourier component, $\tilde{\mathbf{n}}(q, t)$, and will converge at the same rate as $\tilde{\mathbf{n}}(q, t)$. Let us also choose variation without a purely temporal component ($g(t) = 0$), for I wish to emphasize that, even in the absence of purely temporal variation, a change in variation may still produce a change in $\langle n_j \rangle_{x,t}$, and so there will be both global and local convergence processes.

The finite growth rates of perturbations $\tilde{\mathbf{u}}$ and $\boldsymbol{\eta}$ are given by the dominant eigenvalues of \mathbf{B}_u and \mathbf{B}_η : $\lambda_1(\mathbf{B}_u)$ and $\lambda_1(\mathbf{B}_\eta)$. That is, for larger t , $\boldsymbol{\eta}(t) \propto \lambda_1^t(\mathbf{B}_\eta)\boldsymbol{\eta}(0)$ and $\tilde{\mathbf{u}}(q, t) \propto \lambda_1^t(\mathbf{B}_u)\tilde{\mathbf{u}}(q, 0)$, and because $\mathbf{u}(x, t)$ can be represented by a single spatial Fourier component, $\mathbf{u}(x, t) \propto \lambda_1^t(\mathbf{B}_u)\mathbf{u}(x, 0)$. Numerical evidence shows that this system is stable at all spatial frequencies—there is nothing akin to a diffusive instability—and so the dominant eigenvalues must be less than 1. However, the closer the eigenvalues are to 1, the longer it takes for the perturbations to fade away and the longer the transients last.

We have represented $\mathbf{n}(x, t)$ by its spatiotemporal average plus the perturbations $\mathbf{u}'(x, t)$ and $\boldsymbol{\eta}'(t)$ (Eq. 4). Therefore, the transient portion of $\mathbf{n}(x, t)$, $\mathbf{n}(x, t) - \mathbf{n}_s(x, t)$, is proportional to $\lambda_1^t(\mathbf{B}_u)\mathbf{u}(x, 0) + \lambda_1^t(\mathbf{B}_\eta)\boldsymbol{\eta}(0)$. That is, \mathbf{n} 's convergence is the sum of a local convergence process ($\lambda_1^t(\mathbf{B}_u)\mathbf{u}(x, 0)$) and a global one ($\lambda_1^t(\mathbf{B}_\eta)\boldsymbol{\eta}(0)$). Clearly, whichever eigenvalue is larger will dominate \mathbf{n} 's convergence at later times. However, initial conditions also play a role. If, say, the spatially averaged populations are close to their eventual values ($\boldsymbol{\eta}(0)$ is small) but the distributions of high- and low-density areas are far from their eventual forms ($\|\mathbf{u}(x, 0)\|$ is large), then the local redistribution of the populations may initially dominate \mathbf{n} 's convergence ($\|\mathbf{n}(x, t) - \mathbf{n}_s(x, t)\| \sim \lambda_1^t(\mathbf{B}_u)$) even if \mathbf{n} 's conver-

gence ultimately follows that of the total population ($\|\mathbf{n}(x, t) - \mathbf{n}_s(x, t)\| \sim \lambda_1^t(\mathbf{B}_\eta)$). (Distance measure $\|\cdot\|$ is defined in the caption for Fig. 1.)

Examples can be seen in Figs. 1 and 2. In Fig. 1, extremely long-range dispersal ($a_a = a_p = 100$) allows the populations to rapidly redistribute themselves, and this, combined with moderately long-range competition ($b_{aa} = b_{pp} = b_{ap} = 8$), causes there to be little variation in population density from place to place. We might expect, therefore, that local convergence would occur rapidly, and this is confirmed by the small dominant eigenvalue ($\lambda_1(\mathbf{B}_u) = 0.50$). Convergence of the spatially averaged populations, on the other hand, is slower: $\lambda_1(\mathbf{B}_\eta) = 0.84$. When $\langle \mathbf{n} \rangle_x$ begins at 20% above the long-term spatiotemporal average, $\langle \mathbf{n} \rangle_{x,t}$, then \mathbf{n} 's convergence follows the global convergence process described by $\lambda_1(\mathbf{B}_\eta)$, apart from a brief initial amplification of the perturbation. However, when $\langle \mathbf{n} \rangle_x$ begins at $\langle \mathbf{n} \rangle_{x,t}$, then $\boldsymbol{\eta}(x, 0)$ is small and the local convergence process initially dominates \mathbf{n} 's convergence: $\|\mathbf{n} - \mathbf{n}_s\|$ initially vanishes as $\lambda_1^t(\mathbf{B}_u)$, then crosses over to vanish as $\lambda_1^t(\mathbf{B}_\eta)$.

In Fig. 2, dispersal and between-species competition are short-range ($a_a = a_p = b_{ap} = 2.5$), while within-species competition is long-range ($b_{aa} = b_{pp} = 10$). When temporal variation is slow, this combination of traits causes populations to become highly aggregated in favorable areas (Snyder 2008). This, then, is a case where local convergence may involve significant movement of populations, which travel slowly because of restricted dispersal. Local redistribution is slower than overall changes in population levels, and this is reflected in the eigenvalues: ($\lambda_1(\mathbf{B}_u) = 0.94$) > ($\lambda_1(\mathbf{B}_\eta) = 0.84$). Here, beginning with $\langle \mathbf{n} \rangle_x = 10\langle \mathbf{n} \rangle_{x,t}$ allows the global convergence process to dominate briefly: $\|\mathbf{n} - \mathbf{n}_s\|$ initially vanishes as $\lambda_1^t(\mathbf{B}_\eta)$ but then crosses over to vanish as $\lambda_1^t(\mathbf{B}_u)$. If $\langle \mathbf{n} \rangle_x$ starts at $\langle \mathbf{n} \rangle_{x,t}$, \mathbf{n} 's convergence is entirely determined by the local convergence process.

Real variation is, of course, unlikely to be sinusoidal. What happens if the environment varies in a more complicated way, perhaps stochastically? The local convergence process is the sum of convergence processes at all spatial frequencies, each of which proceeds at its own rate. Environmental stochasticity can be analyzed by finding its spectrum and considering the convergence process at each spatial frequency separately. Small-scale redistributions happen quickly while large-scale redistributions take more time. Large-scale redistributions are likely to dominate the local convergence process, both because they take longer and because if variation is positively correlated in space, then there is typically more variation present at large scales than at small (e.g., spatial “red noise”). Figure 3 shows con-

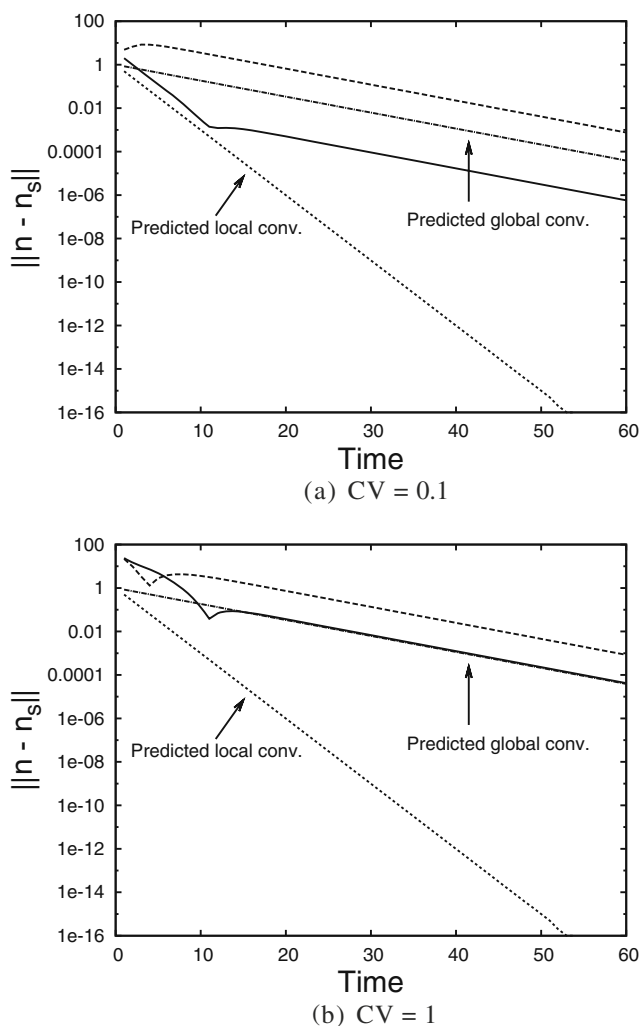


Fig. 1 Distance of $\mathbf{n}(x, t)$ from its stationary distribution (\mathbf{n}_s) vs time for long-range dispersal and competition. **a** Small environmental variation (coefficient of variation (CV) = 0.1) and **b** large environmental variation (CV = 1). $\|\mathbf{n} - \mathbf{n}_s\| = \sqrt{\sum_{j=1}^2 (n_j(x_0, t) - n_{j_s}(x_0, t))^2}$ (i.e., the L_2 norm at an arbitrarily chosen point x_0), where $n_{j_s}(x, t)$ is the stationary distribution for species j and x_0 is a point far from the boundaries of the system. *Dash-dot line*: predicted global convergence rate; *dotted line*: predicted local convergence rate. Y intercepts are arbitrary. *Dashed line*: \mathbf{n} starting with $\langle \mathbf{n} \rangle_x = 1.2 \langle \mathbf{n} \rangle_{x,t}$; *solid line*: \mathbf{n} starting with $\langle \mathbf{n} \rangle_x = \langle \mathbf{n} \rangle_{x,t}$. When the populations begin with their spatial averages 20% above their eventual spatiotemporal averages (*dashed line*), the global convergence process dominates, and \mathbf{n} converges at the same rate as $\langle \mathbf{n} \rangle_x$. When the populations begin with their spatial averages equal to their eventual spatiotemporal averages (*solid line*), the local convergence process initially dominates as the populations redistribute themselves, so that \mathbf{n} initially converges at the local convergence rate, then crosses over to converge at the global convergence rate. $a_a = a_p = 100$, $b_{11} = b_{22} = b_{12} = 8$, $\epsilon_a(x, t) = 0.1 \sin(2\pi x/32) \sin(2\pi t/32) = -\epsilon_p(x, t)$. (Sinusoidal variation in time was chosen simply to make it easier to determine the stationary distribution.) The remaining parameter values are listed and discussed at the end of the “Model” section. Convergence rates for \mathbf{n} were determined by numerically integrating the model equations, using no approximations

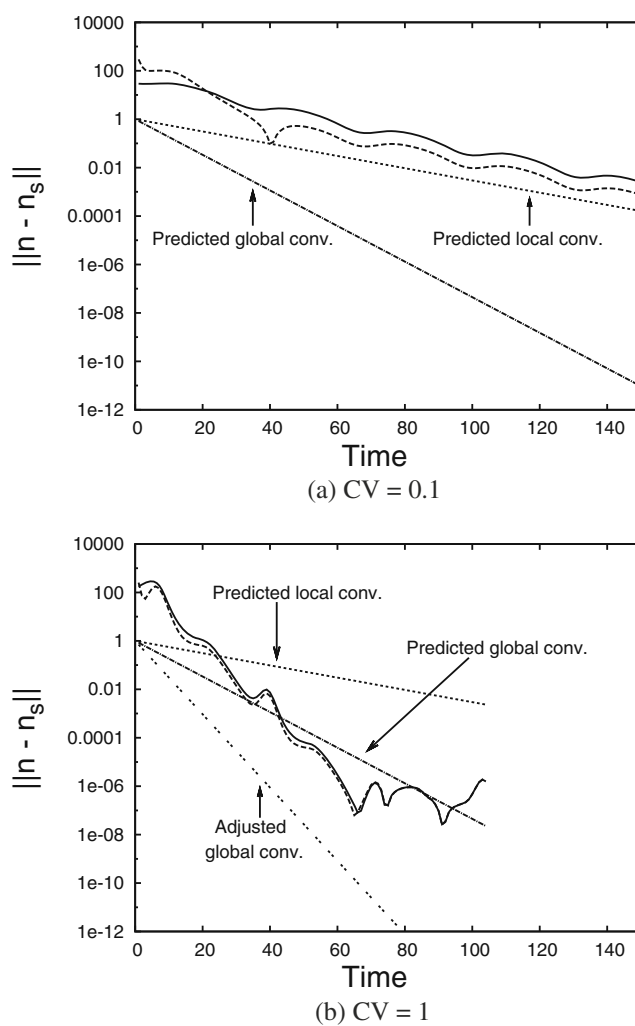


Fig. 2 Distance of $\mathbf{n}(x, t)$ from its stationary distribution (\mathbf{n}_s) vs time for short-range dispersal and between-species competition and long-range within-species competition. **a** Small environmental variation (CV = 0.1) and **b** large environmental variation (CV = 1). *Dash-dot line*: predicted global convergence rate; *dotted line*: predicted local convergence rate; *double-dot line* (part b): predicted global convergence rate using observed $\langle \mathbf{n} \rangle_{x,t}$ (“Adjusted global conv.”). Y intercepts are arbitrary. *Dashed line*: \mathbf{n} starting with $\langle \mathbf{n} \rangle_x = 10 \langle \mathbf{n} \rangle_{x,t}$; *solid line*: \mathbf{n} starting with $\langle \mathbf{n} \rangle_x = \langle \mathbf{n} \rangle_{x,t}$. When the populations begin with their spatial averages ten times above their eventual spatiotemporal averages (*dashed line*), the global convergence process initially dominates as the total population drops, so that \mathbf{n} converges at the global convergence rate until roughly time 40, then crosses over to converge at the local convergence rate. When the populations begin with their spatial averages equal to their eventual spatiotemporal averages (*solid line*), the local convergence process dominates, and \mathbf{n} converges at the same rate as \mathbf{u} . $a_a = a_p = b_{12} = 2.5$, $b_{11} = b_{22} = 10$, $\epsilon_a(x, t)$ and $\epsilon_p(x, t)$ as in Fig. 1. Convergence rates for \mathbf{n} were determined by numerically integrating the model equations, using no approximations

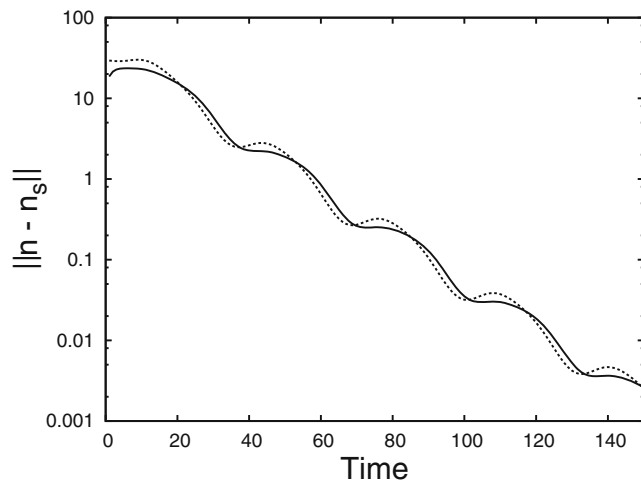


Fig. 3 Distance of $\mathbf{n}(x, t)$ from its stationary distribution (\mathbf{n}_s) vs time in the presence of spatial variation at two frequencies. The *solid line* shows $\|\mathbf{n}(x, t) - \mathbf{n}_s\|$ when spatial variation is present in equal amounts at period 32 and period 16 ($\epsilon(x, t) \propto \sin(2\pi t/32) [\sin(2\pi x/32) + \sin(2\pi x/16)]$), and the *dotted line* shows convergence when variation is present only at period 32. Convergence when spatial variation has periods 32 and 8 (not shown) is not visibly different from convergence at periods 32 and 16. Parameters are the same as for Fig. 2

vergence rates when environmental variation is present in equal amounts with spatial periods 32 and 16, 32 and 8, or only 32. The convergence rates are essentially identical.

What happens if environmental variation is not small? After all, some disturbances are extreme, and in such cases, we might expect linear analysis to break down. The answer depends on the size of the resulting population variation. Figures 1b and 2b show the same convergence processes as in parts a but with fecundity varying between zero and twice its mean instead of $\pm 10\%$ of the mean. In Fig. 1b, long-range dispersal and competition ensure that population variation about the current mean remains moderate, and as a result, the convergence rates predicted by the eigenvalues remain good. In Fig. 2b, on the other hand, dispersal and competition parameters cause population densities to be very sensitive to environmental variation, and the large fluctuations in fecundity cause large variation in population density. Here, the eigenvalues do a poor job of predicting convergence rates, but this is not entirely the fault of linearization. The variation in population density causes our $O(\sigma^0)$ prediction for $\langle \mathbf{n} \rangle_{x,t}$ to be off, but if we substitute the observed value for $\langle \mathbf{n} \rangle_{x,t}$, the linearized dynamics continue to predict convergence rates well. I conjecture that using a higher-order prediction for $\langle \mathbf{n} \rangle_{x,t}$ within a linear analysis of the transient dynamics may provide reasonably accurate results.

Discussion

In summary, the convergence of a population to a new distribution following a change in disturbance regime or any other pattern of environmental variation can be separated into a global convergence process and a local convergence process. The global convergence process describes how the total or spatially averaged populations reach their new levels. This is the process that governs whether a change in environmental variation will lead to extinction. The local convergence process describes how the populations redistribute themselves into their new pattern of high- and low-density areas, relative to the current means. This is the process that governs how a change in environmental variation will affect local crowding or spatial segregation. Both processes are important in describing how an individual's competitive environment changes following a change in environmental variation. This paper has shown that global and local convergence may occur on very different time scales and that either one may be slower. While the slower process governs the populations' convergence at later times, the faster process may initially dominate if it starts further from its stationary distribution than the slower process. In such a case, the population will converge to its new distribution relatively quickly at first and then slow down.

To understand how populations adjust to a change in environmental variation, I have treated the population distribution just after the change as a perturbation away from the new distribution. However, the analysis presented in Section “Analysis” applies equally well to populations recovering to their original distributions after a single disturbance. In this context, transient duration can be thought of as recovery time and convergence rate as resilience. Various empirical studies have measured resilience without considering spatial distribution (Steinman et al. 1991; Mulholland et al. 1991; Steinman et al. 1992; Wassenaar et al. 2005), but for communities where local interactions are important, such as plant communities, I argue that population distributions, and not just total population sizes, need to recover for population dynamics to return to their predisturbance form. This paper shows that when disturbances are spatially heterogeneous, the resilience of population distributions depends on initial conditions. If researchers estimate resilience based on a system's initial response to a perturbation, some initial conditions may give an overly optimistic estimate of recovery rate. Alternatively, it may be that, after the initial rapid convergence, the population structure is so close to its eventual form that further convergence has few practical consequences. If so, resilience estimates based on

short time series will be accurate but only for certain initial conditions.

I suspect that modeling is the only way to be certain that an observed convergence rate is the ultimate convergence rate. That said, the conclusions in this paper seem likely to be general: for highly aggregated distributions (typically produced by short-range dispersal), local convergence is likely to be slower than global convergence, while for more nearly uniform distributions, global convergence is likely to be slower. If local convergence is slower, then initial conditions in which the total population size is far from its eventual value may cause convergence to follow the faster global convergence rate before crossing over to the local convergence rate. Similarly, if global convergence is slower, then initial conditions in which the population distribution is far from its eventual form may cause the faster local convergence rate to dominate initially.

This paper has focused on a one-time change in environmental variation, such as that which might occur with habitat fragmentation or the introduction or cessation of grazing. These represent a shift from one stationary pattern of variation to a different stationary pattern. However, some changes occur continuously. Global climate change, for example, produces trends in climate data, so that environmental variation is never stationary. Population responses to nonstationary variation are difficult to analyze, but we can hope that populations converge quickly relative to the time scale

of the trend, so that populations are always in “equilibrium” with the current environment. The analysis presented in this paper allows us to determine the validity of this assumption.

This paper has focused on how local and global convergence processes affect transient duration after a change in environmental variation. It will also be important to understand when we should expect long transients, what transient behavior may be like, and what the community consequences will be. These are the subject of current work and papers in preparation.

Acknowledgements This work was supported by start-up funds from Case Western Reserve University.

Appendix

Here, I linearize the dynamics of the annual. Linearization for the perennial proceeds in similar fashion. As in the “Analysis” section, let us write $n_a(x, t) = \langle n_a \rangle_{x,t} (1 + \eta'_a(t) + u'_a(x, t))$. If we were interested in the dynamics of $\eta'_a(t)$ and $u'_a(x, t)$ (stationary distributions plus transients), we would need \mathbf{B}_ϵ and \mathbf{B}_Ω and so would have to reexpress $E_a(x, t)$ in terms of perturbations $\epsilon_a(x, t)$ and $\Omega_a(t)$. However, as discussed in the “Analysis” section, the transient dynamics depend only on \mathbf{B}_u and \mathbf{B}_η , so we can let $E_a(x, t) = \langle E_a \rangle_{x,t}$. Thus, we rewrite Eq. 1 as

$$\begin{aligned} & \langle n_a \rangle_{x,t} (1 + \eta'_a(t + 1) + u'_a(x, t + 1)) \\ &= k_a * \left[\frac{\langle E_a \rangle_{x,t} g_a \langle n_a \rangle_{x,t} (1 + \eta'_a(t) + u'_a(x, t))}{\gamma_{ap} \langle n_p \rangle_{x,t} (1 + \eta'_p(t) + (U_{ap} * u'_p)(x, t)) + \gamma_{aa} g_a \langle n_a \rangle_{x,t} (1 + \eta'_a(t) + (U_{aa} * u'_a)(x, t))} \right] \\ & \quad + s_a (1 - g_a) \langle n_a \rangle_{x,t} (1 + \eta'_a(t) + u'_a(x, t)) \end{aligned} \tag{8}$$

Suppressing dependence on x and t for conciseness, we Taylor expand the right-hand side to first order in u' and η' to obtain

$$\begin{aligned} & 1 + \eta'_a + u'_a \\ &= \frac{\langle E_a \rangle_{x,t} g_a}{d} \left[1 + \eta'_a - \frac{\gamma_{ap} \langle n_p \rangle_{x,t} \eta'_p}{d} - \frac{\gamma_{aa} g_a \langle n_a \rangle_{x,t} \eta'_a}{d} \right. \\ & \quad \left. + k_a * \left(u'_a - \frac{\gamma_{ap} \langle n_p \rangle_{x,t} U_{ap} * u'_p}{d} - \frac{\gamma_{aa} g_a \langle n_a \rangle_{x,t} U_{aa} * u'_a}{d} \right) \right] \\ & \quad + s_a (1 - g_a) \langle n_a \rangle_{x,t} (1 + \eta'_a + u'_a), \end{aligned} \tag{9}$$

where $d = \gamma_{ap} \langle n_p \rangle_{x,t} + \gamma_{aa} g_a \langle n_a \rangle_{x,t}$.

If we were to take the spatial average of this equation, all terms with a u' would vanish, since $\langle u' \rangle_x = 0$, and we would be left with an equation for η'_a . Subtracting this equation from both sides, we are left with an equation for u'_a . We see, then, that the linearized dynamics of u'_a and η'_a are independent. Subtracting off the constant terms (which are the equation for $\langle n_a \rangle_{x,t}$) and writing separate equations for η'_a and u'_a , we obtain

$$\begin{aligned} \eta'_a &= \left[\frac{\langle E_a \rangle_{x,t} g_a}{d} \left(1 - \frac{\gamma_{aa} g_a \langle n_a \rangle_{x,t}}{d} \right) + s_a (1 - g_a) \right] \eta'_a \\ & \quad - \frac{\langle E_a \rangle_{x,t} g_a \gamma_{ap} \langle n_p \rangle_{x,t}}{d} \eta'_p \end{aligned} \tag{10}$$

and

$$u'_a = \frac{\langle E_a \rangle_{x,t} g_a}{d} k_a * \left[u'_a - \frac{\gamma_{aa} g_a \langle n_a \rangle_{x,t}}{d} U_{aa} * u'_a \right] + s_a (1 - g_a) u'_a - \frac{\langle E_a \rangle_{x,t} g_a}{d} \frac{\gamma_{ap} \langle n_p \rangle_{x,t}}{d} k_a * U_{ap} * u'_p. \tag{11}$$

At this point, we take the spatial Fourier transform of the equation for u'_a . The Fourier transform of a convolution is a product of Fourier transforms (e.g., the Fourier transform of $U_{aa} * u'_a$ is $\tilde{U}_{aa} \tilde{u}'_a$), and so by transforming, we move from an equation where the dynamics at one location depend on the populations at all other locations to an equation where the dynamics at one frequency depend only on the populations at that frequency. It is this step that allows our dynamical system to decouple into a set of independent matrix models at different spatial frequencies.

Finally, we can simplify these expressions somewhat by noting that, to $O(\sigma)$,

$$\langle n_a \rangle_{x,t} = \frac{\langle E_a \rangle_{x,t} g_a \langle n_a \rangle_{x,t}}{\gamma_{ap} \langle n_p \rangle_{x,t} + \gamma_{aa} g_a \langle n_a \rangle_{x,t}} + s_a (1 - g_a) \langle n_a \rangle_{x,t}, \tag{12}$$

and thus,

$$\frac{\langle E_a \rangle_{x,t} g_a}{\gamma_{ap} \langle n_p \rangle_{x,t} + \gamma_{aa} g_a \langle n_a \rangle_{x,t}} \equiv \frac{\langle E_a \rangle_{x,t} g_a}{d} = 1 - s_a (1 - g_a). \tag{13}$$

Letting $D_a = s_a (1 - g_a)$, we arrive at our final expressions:

$$\eta'_a(t+1) = \underbrace{\left[(1 - D_a) \left(1 - (1 - D_a) \frac{\gamma_{aa} \langle n_a \rangle_{x,t}}{\langle E_a \rangle_{x,t}} \right) + D_a \right]}_{\mathbf{B}_{\eta_{11}}} \eta'_a(t) + \underbrace{\left[- (1 - D_a)^2 \frac{\gamma_{ap} \langle n_p \rangle_{x,t}}{g_a \langle E_a \rangle_{x,t}} \right]}_{\mathbf{B}_{\eta_{12}}} \eta'_p(t) \tag{14}$$

$$\begin{aligned} \tilde{u}'_a(q, t+1) &= \underbrace{\left[(1 - D_a) \tilde{k}_a(q) \left(1 - (1 - D_a) \tilde{U}_{aa}(q) \frac{\gamma_{aa} \langle n_a \rangle_{x,t}}{\langle E_a \rangle_{x,t}} \right) + D_a \right]}_{\mathbf{B}_{u_{11}}} \\ &\times \tilde{u}'_a(q, t) + \underbrace{\left[- (1 - D_a)^2 \tilde{k}_a(q) \tilde{U}_{ap}(q) \frac{\gamma_{ap} \langle n_p \rangle_{x,t}}{g_a \langle E_a \rangle_{x,t}} \right]}_{\mathbf{B}_{u_{12}}} \\ &\times \tilde{u}'_p(q, t). \end{aligned} \tag{15}$$

We can find the linearized dynamics of the perennial in the same fashion, obtaining

$$B_{u_{11}}(q) = (1 - D_a) \tilde{k}_a(q) \times \left[1 - (1 - D_a) \tilde{U}_{aa}(q) \frac{\gamma_{aa} \langle n_a \rangle_{x,t}}{\langle E_a \rangle_{x,t}} \right] + D_a \tag{16}$$

$$B_{u_{12}}(q) = - (1 - D_a)^2 \tilde{k}_a(q) \tilde{U}_{ap}(q) \frac{\gamma_{ap} \langle n_p \rangle_{x,t}}{g_a \langle E_a \rangle_{x,t}} \tag{17}$$

$$B_{u_{21}}(q) = - (1 - s_p)^2 \tilde{k}_p(q) \tilde{U}_{pa}(q) \frac{\gamma_{pa} g_a \langle n_a \rangle_{x,t}}{g_p \langle E_p \rangle_{x,t}} \tag{18}$$

$$B_{u_{22}}(q) = (1 - s_p) \tilde{k}_p(q) \times \left[1 - (1 - s_p) \tilde{U}_{pp}(q) \frac{\gamma_{pp} \langle n_p \rangle_{x,t}}{g_p \langle E_p \rangle_{x,t}} \right] + s_p \tag{19}$$

and

$$B_{\eta_{11}} = (1 - D_a) \left[1 - (1 - D_a) \frac{\gamma_{aa} \langle n_a \rangle_{x,t}}{\langle E_a \rangle_{x,t}} \right] + D_a \tag{20}$$

$$B_{\eta_{12}} = - (1 - D_a)^2 \frac{\gamma_{ap} \langle n_p \rangle_{x,t}}{g_a \langle E_a \rangle_{x,t}} \tag{21}$$

$$B_{\eta_{21}} = - (1 - s_p)^2 \frac{\gamma_{pa} g_a \langle n_a \rangle_{x,t}}{g_p \langle E_p \rangle_{x,t}} \tag{22}$$

$$B_{\eta_{22}} = (1 - s_p) \left[1 - (1 - s_p) \frac{\gamma_{pp} \langle n_p \rangle_{x,t}}{g_p \langle E_p \rangle_{x,t}} \right] + s_p. \tag{23}$$

References

Abrams MD (1982) Fire and the development of oak forests. *Bioscience* 42:346–353

Adler P, HilleRisLambers J, Kyriakidis P, Guan Q, Levine J (2006) Climate variability has a stabilizing effect on the coexistence of prairie grasses. *Proc Natl Acad Sci U S A* 103:12793–12798

Beddington J, Free C, Lawton J (1976) Concepts of stability and resilience in predator-prey models. *J Anim Ecol* 45:791–816

Borer ET, Hosseini PR, Seabloom EW, Dobson AP (2007) Pathogen-induced reversal of native dominance in a grassland community. *Proc Natl Acad Sci U S A* 104:5473–5478

Chesson P (1994). Multispecies competition in variable environments. *Theor Popul Biol* 45:227–276

Chesson P (2000) General theory of competitive coexistence in spatially-varying environments. *Theor Popul Biol* 58:211–237

Chesson P, Gebauer RL, Schwinning S, Huntly N, Wiegand K, Ernest MS, Sher A, Novoplansky A, Weltzin JF (2004) Resource pulses, species interactions, and diversity maintenance in arid and semi-arid environments. *Oecologia* 141:236–253

Dettmers R (2003) Status and conservation of shrubland birds in the northeastern US. *For Ecol Manag* 185:81–93

Harrison G (1979) Stability under environmental stress: resistance, resilience, persistence, and variability. *Am Nat* 113: 659–669

- Law R, Dieckmann U (2000) A dynamical system for neighborhoods in plant communities. *Ecology* 81:2137–2148
- Litvaitis J (2001) Importance of early successional habitats to mammals in eastern forests. *Wildl Soc Bull* 29:466–473
- Mack M, D'Antonio C (1998) Impacts of biological invasions on disturbance regimes. *Trends Ecol Evol* 13:195–198
- Mulholland PJ, Steinman AD, Palumbo AV, DeAngelis DL, Flum TE (1991) Influence of nutrients and grazing on the response of stream periphyton communities to a scour disturbance. *J North Am Benthol Soc* 10:127–142
- Rees M, Grubb P, Kelly D (1996) Quantifying the impact of competition and spatial heterogeneity on the structure and dynamics of a four-species guild of winter annuals. *Am Nat* 147:1–32
- Seabloom EW, van der Valk AG (2003) The development of vegetative zonation patterns in restored prairie potholes. *J Appl Ecol* 40:92–100
- Seabloom EW, Harpole WS, Reichman O, Tilman D (2003) Invasion, competitive dominance, and resource use by exotic and native california grassland species. *Proc Natl Acad Sci U S A* 100:13384–13389
- Silvertown J, Holtier S, Johnson J, Dale P (1992) Cellular automaton models of interspecific competition for space—the effect of pattern on process. *J Ecol* 80:527–534
- Snyder RE (2007) Spatiotemporal population distributions and their implications for species coexistence in a variable environment. *Theor Popul Biol* 72:7–20
- Snyder RE (2008) When does environmental variation most influence species coexistence? *Theor Ecol* 1:129–139
- Snyder RE, Chesson P (2004) How the spatial scales of dispersal, competition, and environmental heterogeneity interact to affect coexistence. *Am Nat* 164:633–650
- Steinman AD, Mulholland PJ, Palumbo AV, Flum TF, DeAngelis DL (1991) Resilience of lotic ecosystems to a light-elimination disturbance. *Ecology* 72:1299–1313
- Steinman AD, Mulholland PJ, Palumbo AV, DeAngelis DL, Flum TE (1992) Lotic ecosystem response to a chlorine disturbance. *Ecol Appl* 2:341–355
- Stoll P, Prati D (2001) Intraspecific aggregation alters competitive interactions in experimental plant communities. *Ecology* 82:319–327
- Turnbull LA, Coomes DA, Purves DW, Rees M (2007) How spatial structure alters population and community dynamics in a natural plant community. *J Ecol* 95:79–89
- USGCRP (ed) (2000) Climate change impacts on the United States: the potential consequences of climate variability and change: overview. National Assessment Synthesis Team, U.S. Global Change Research Program, Cambridge University Press, New York
- Wassenaar T, van Aarde R, Pimm S, Ferreira S (2005) Community convergence in disturbed subtropical dune forests. *Ecology* 86:655–666
- Webster J, Waide J, Patten B (1975) Nutrient recycling and the stability of ecosystems. In: Howell F (ed) Mineral cycling in southeastern ecosystems. AEC Symp. Ser. Conf. 74-0513
- Weller M, Spratcher C (1965) Role of habitat in the distribution and abundance of marsh birds. Special report 43, Iowa Agriculture and Home Economics Experiment Station, Ames